RSC Advances

ROYAL SOCIETY OF CHEMISTRY

www.rsc.org/advances

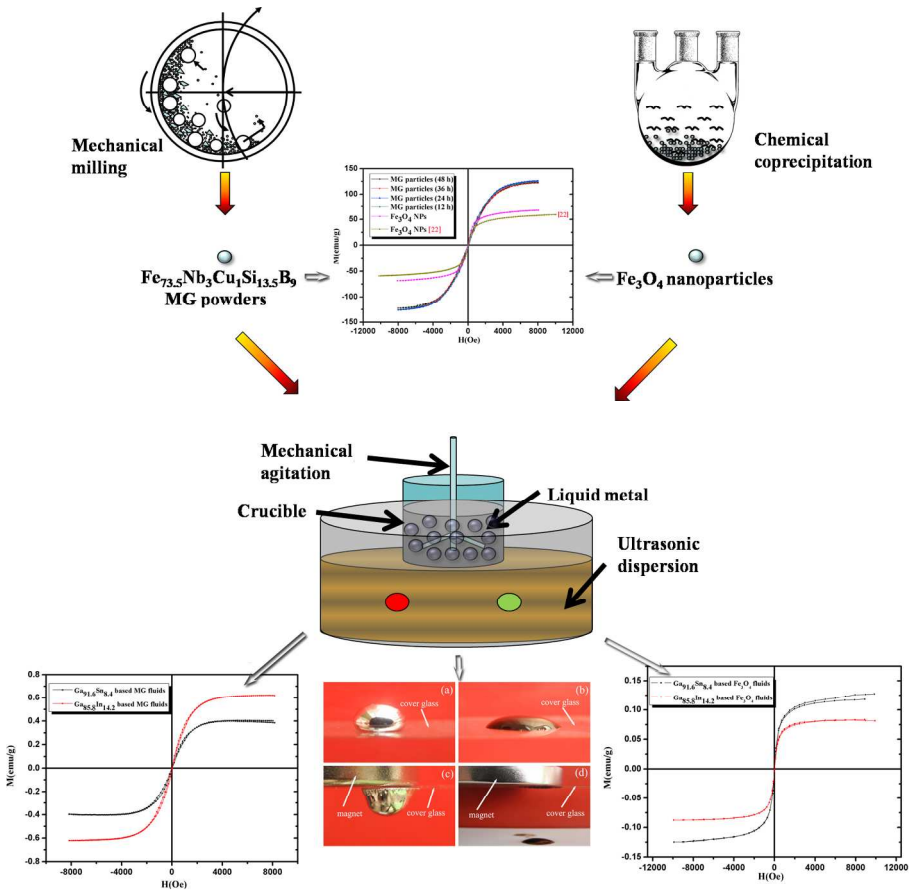

Graphical abstract
173x153mm (300 x 300 DPI)

Metal-based Magnetic Functional Fluids with Amorphous Particles

Chuncheng Yang, Xiufang Bian*, Jingyu Qin, Tongxiao Guo, Xiaolin Zhao

Key Laboratory for Liquid-Solid Structural Evolution and Processing of Materials, Ministry of Education, Shandong University, Jinan 250061, China

Abstract

Two metal-based magnetic functional fluids, Ga-Sn and Ga-In magnetic liquids, were fabricated by doping with $Fe_{73.5}Nb_3Cu_1Si_{13.5}B_9$ metallic glass particles and nanoscale Fe_3O_4 particles, respectively. The saturation magnetization of the metallic glass particles, $Fe_{73.5}Nb_3Cu_1Si_{13.5}B_9$, is about 125 emu/g, nearly 50% larger than that of Fe_3O_4 crystalline particles which are usually used in water-based magnetic fluids. It is discovered that functional fluids, $Ga_{85.8}In_{14.2}$ and $Ga_{91.6}Sn_{8.4}$ alloy liquids, with $Fe_{73.5}Nb_3Cu_1Si_{13.5}B_9$ particles exhibit high saturation magnetization as well as low coercivity and remanence. Furthermore, the magnetic hysteresis curves confirm that the liquid metal-based magnetic functional fluids with $Fe_{73.5}Nb_3Cu_1Si_{13.5}B_9$ particles have higher magnetization than the metal-based Fe_3O_4 fluids. Owing to the high alloy boiling point more than 2000 K, the metal-based functional fluids should be useful materials for engineering applications when the surrounding temperature is relatively high. Interestingly, these functional fluids offer the properties of superior thermal or electrical conductivity over conventional water-based fluids.

Keywords: liquid metal, functional fluid, metallic glass, magnetic property.

Introduction

Magnetic functional fluids have been subjected to extensive studies in the past few decades owing to their unique magnetic properties and fluidity as well as promising potential in

*Corresponding author: Tel: + 86 531 88392748; Fax: + 86 531 88395011.

E-mail address: xfbian@sdu.edu.cn (X.F. Bian).

advanced applications.[1-4] The carrier liquid is a highly significant component of the functional fluid. When selecting a carrier liquid, of significance is the consideration of the melting point, boiling temperature and evaporation rate. Historically, the most widely studied carrier liquids are organic or polar solvents, such as oil, toluene, hexane or water. However, typical organic solvents exhibit relatively high toxicity and volatility. Water-based magnetic controllable fluids have been widely applied in organic tissue cell separation, thermal therapy and drug delivery.[5-7] Unfortunately, they are not useful for applications where the surrounding temperature is relatively high because of the lower boiling temperature of the water-based fluids.[8] Liquid metals, such as gallium and its alloys, have a low melting point, very low evaporation pressure, and an extremely high boiling point of more than 2000 K. In particular, gallium and its alloys have the advantages of remaining in the liquid state over a wide temperature range. These liquid metals exhibit a high electrical and thermal conductivity as well as fluidity. Although the mercury-based magnetic fluids have been investigated,[9] the practical application is rather limited due to its safety issue of serious toxicity. Thus, the environmentally-friendly liquid gallium and its alloys become a good choice for the carrier liquid in a functional fluid. The functional fluids-based on liquid metal formulations may offer the merit of superior thermal or electrical conductivity over the current conventional functional fluids. However, published literatures on this aspect are scarce. Relevant examples are a study of movement of liquid gallium dispersing low concentration of magnetic particles [10] and a recent study of fabrication of magnetic fluid through loading Ni particles into gallium.[11]

Magnetic nanoparticles,[12-14] especially Fe_3O_4 iron oxides, bear many intriguing properties such as superparamagnetism and biocompatibility, which has stimulated great interest and research into magnetic fluids. However, the weak magnetic properties of current functional fluids constrain their practical use in some areas, such as elevated-temperature seals and high temperature cooling applications. The Fe-based metallic glasses (MGs) have broad prospects for industry applications due to low cost of raw materials together with their uniquely high magnetic properties relating to the short-range ordered and long-range disordered atomic

structures.[15,16] Nowadays, the use of ferromagnetic amorphous alloys for efficient transformer cores is becoming more widespread, as they are the most magnetically soft commercially available materials.[17] The Fe-based metallic glass particles have an excellent development potential in the application of magnetic functional fluids. Detailed research of Fe-based MG particles and their soft magnetic properties applied to functional fluids have not been yet significantly reported.

Two metal-based magnetic functional fluids, Ga-Sn and Ga-In magnetic functional liquids, were investigated by doping with $Fe_{73.5}Nb_3Cu_1Si_{13.5}B_9$ metallic glass particles and nanoscale Fe_3O_4 particles, respectively. Ga-Sn eutectic alloy and Ga-In eutectic alloy exhibit low melting points of 20.5 ℃ and 15.3 ℃, respectively.[18] This makes them suitable for selection as carrier liquids. Considering the excellent magnetic properties and fluidity with high thermal and electrical conductivity, these metal-based magnetically controllable fluids could offer opportunities in a variety of emerging applications such as magneto-caloric energy conversion devices,[19] elevated-temperature seals,[20] high temperature cooling applications,[8] as well as printed electronics[21] etc.

Experimental

The Fe_3O_4 nanoparticles were synthesized by a chemical co-precipitation method. The black Fe_3O_4 nanoparticles were obtained using the following reaction:

$$2Fe^{3+}+Fe^{2+}+8NH_3\bullet H_2O=Fe_3O_4+8NH_4^{+}+4H_2O$$

The $Fe_{73.5}Nb_3Cu_1Si_{13.5}B_9$ MG ribbons were prepared by melting, then spinning. The ribbons were milled 12h, 24h, 36h and 48h with a rotation speed of 360r/min while using a high purity Ar gas protection shield to obtain the $Fe_{73.5}Nb_3Cu_1Si_{13.5}B_9$ MG powders. The samples of $Ga_{85.8}In_{14.2}$ and $Ga_{91.6}Sn_{8.4}$ liquid metal alloys used as base fluids in this study were prepared with pure Ga, In and Sn of 99.99% purity.

Certain amounts of Ga, In, and Sn metals were weighed and melted to obtain the $Ga_{85.8}In_{14.2}$ and $Ga_{91.6}Sn_{8.4}$ liquid metals. Then appropriate Fe_3O_4 nanoparticles and $Fe_{73.5}Nb_3Cu_1Si_{13.5}B_9$

MG particles were added to the liquid metal. Next, the mixed fluids were stirred constantly by mechanical stirring and supersonic dispersion in air at room temperature. It has been found that the wettability and compatibility of gallium and its alloys with various materials can be improved with a slight oxidization processing.[11] With vigorous stirring, more and more $Ga_{85.8}In_{14.2}$ and $Ga_{91.6}Sn_{8.4}$ liquid metal were oxidized. The Fe_3O_4 nanoparticles and $Fe_{73.5}Nb_3Cu_1Si_{13.5}B_9$ MG particles were gradually mixed uniformly within the liquid metal. Here liquid metal alloys and magnetic particles were physically blended and compatible with each other. Figure. 1 displays the schematic of preparation processing of the liquid metal-based functional fluids. Metal-based magnetic functional fluids with a mass fraction of 2%, by doping with $Fe_{73.5}Nb_3Cu_1Si_{13.5}B_9$ particles and Fe_3O_4 nanoparticles were prepared, respectively.

Results and discussion

Figure. 2 shows the SEM (scanning electron microscope) images of the $Fe_{73.5}Nb_3Cu_1Si_{13.5}B_9$ MG powders. The MG particle size reduces with increasing milling time. The particle size of the MG particles is 10-50 um after being milled 12 hours. However, the size of MG particles could reach 2-8 um or smaller after being milled 48 hours.

The EDX (energy dispersive X-ray) spectrograms of $Fe_{73.5}Nb_3Cu_1Si_{13.5}B_9$ MG ribbons and particles after being milled for 48 hours are shown in Figure. 3, which indicates that elements of MG ribbons and particles are almost the same.

The XRD (X-ray diffraction) patterns of Fe_3O_4 nanoparticles and $Fe_{73.5}Nb_3Cu_1Si_{13.5}B_9$ particles are shown in Figure. 4. It indicates a series of diffraction peaks for (220), (311), (400), (422), (511) and (440) planes, which are related to Fe_3O_4 phase [JCPDS card No. 84-1436]. No obvious impurity peaks can be observed. Typical broad peaks are found for the $Fe_{73.5}Nb_3Cu_1Si_{13.5}B_9$ particles at about $2\theta = 45°$. No distinct diffraction peaks corresponding to crystalline phases are observed, which verifies that all $Fe_{73.5}Nb_3Cu_1Si_{13.5}B_9$ particles after being milled, are still amorphous.

The DSC (differential scanning calorimeters) curves of the $Fe_{73.5}Nb_3Cu_1Si_{13.5}B_9$ particles at a

heating rate of 20K/min are shown in Figure. 5. Two exothermic peaks during heating indicate two stages crystallization of the ribbons and powders. The two peaks reveal that the particles remain amorphous even after being milled for 48 h. The results correspond well with the XRD patterns of $Fe_{73.5}Nb_3Cu_1Si_{13.5}B_9$ particles as mentioned above.

The magnetic properties of Fe_3O_4 nanoparticles and $Fe_{73.5}Nb_3Cu_1Si_{13.5}B_9$ MG particles after being milled have been investigated by using a vibrating sample magnetometer (VSM) at room temperature. The results in Figure. 6 show that the saturation magnetization of the Fe_3O_4 nanoparticles is about 68 emu/g. Zero remanence and zero coercivity indicate that the Fe_3O_4 particles have superparamagnetism. There has not been a significant change in saturation magnetization of the $Fe_{73.5}Nb_3Cu_1Si_{13.5}B_9$ MG particles before or after being milled as shown in Figure 6 (a) and (b). However, the value is about 124.2 emu/g, which is two times larger than that of the Fe_3O_4 nanoparticles shown in reference.[22] The $Fe_{73.5}Nb_3Cu_1Si_{13.5}B_9$ MG particles have relatively high saturation magnetization compared with various types of ferrite such as Ni-Zn and Mn-Zn ferrite etc.[23,24]

The hysteresis curves of liquid metal-based magnetic functional fluids with Fe_3O_4 nanoparticles and $Fe_{73.5}Nb_3Cu_1Si_{13.5}B_9$ MG particles are shown in Figure. 7. As for the $Ga_{85.8}In_{14.2}$ and $Ga_{91.6}Sn_{8.4}$-based $Fe_{73.5}Nb_3Cu_1Si_{13.5}B_9$ fluids, both of them exhibit good magnetization, which indicates that the MG particles have good compatibility with the liquid metal. The saturation magnetization of $Ga_{91.6}Sn_{8.4}$-based magnetic functional fluids is about 0.4 emu/g, as shown in Figure. 7(a), while the corresponding value is about 0.6 emu/g for the $Ga_{85.8}In_{14.2}$-based magnetic functional fluids. Both of $Ga_{91.6}Sn_{8.4}$ and $Ga_{85.8}In_{14.2}$-based magnetic functional fluids have relatively low coercivity and remanence as shown in Table. 1.

The magnetic properties of $Ga_{85.8}In_{14.2}$ and $Ga_{91.6}Sn_{8.4}$-based Fe_3O_4 magnetic fluids were also investigated as shown in Figure. 7 (b). It can be seen that both of $Ga_{85.8}In_{14.2}$ and $Ga_{91.6}Sn_{8.4}$-based Fe_3O_4 magnetic fluids exhibit superparamagnetism with saturation magnetization of 0.08 emu/g and 0.13 emu/g, respectively. Almost zero remanence and zero coercivity can be observed. The saturation magnetization of $Ga_{91.6}Sn_{8.4}$-based Fe_3O_4 magnetic fluid is higher

than that of $Ga_{85.8}In_{14.2}$-based Fe_3O_4 magnetic fluid.

Controlled manipulation of small volumes of functional liquid, as either flow or droplets, is extremely important in miniaturized systems for chemical and biological applications, such as purification and high-throughput microarrays analysis.[25] To further evaluate the magnetic effects of the liquid metal-based fluids, experiments on the behavior of fluid droplets were performed. A fluid droplet of a water-based Fe_3O_4 magnetic fluid with a mass fraction of 2% was also tested for comparison. The fluid droplets of water-based fluids and $Ga_{85.8}In_{14.2}$-based magnetic functional fluids with $Fe_{73.5}Nb_3Cu_1Si_{13.5}B_9$ MG particles were placed on the cover glass, respectively. The behaviors of the droplets are shown in Figure. 8. Figure. 8(a)-(b) are the droplets without the magnetic field being present. At initial conditions, the MG particles were mixed uniformly within the $Ga_{85.8}In_{14.2}$ liquid metal as shown in Figure. 8(a). Using a permanent magnet, we are able to observe the basic features of the droplet behavior. From Figure. 8(c) we can see that the whole droplet of the $Ga_{85.8}In_{14.2}$-based fluids could be attracted upwards onto the cover glass by the permanent magnet, while the water based droplet suffered component separation by the interplay between the magnetic and gravitational forces as shown in Figure. 8(d). The results demonstrate that the liquid metal-based functional fluids with MG particles exhibit better magnetic properties over conventional water-based Fe_3O_4 magnetic fluids. As magnetic droplets can be assembled into well-defined geometric patterns under equilibrium conditions, this droplet methodology of liquid metal-based functional fluids would have potential application to droplet-based microfluidics and possibly e-paper technology. The magnetic parameters of all $Ga_{91.6}Sn_{8.4}$ and $Ga_{85.8}In_{14.2}$-based magnetic functional fluids can be seen in Table. 1.

The temperature dependent magnetization properties of the metal-based MG functional fluids have been investigated using Superconducting Quantum Interference Device. Figure. 9 shows the magnetization curves of (a) $Fe_{73.5}Nb_3Cu_1Si_{13.5}B_9$ MG particles, (b) $Ga_{85.8}In_{14.2}$ based MG fluids and (c) $Ga_{91.6}Sn_{8.4}$ based MG fluids, measured between 293 K and 333 K in 10 K steps. From figure. 9(a), it can be seen that the magnetization value of the MG particles decreases with increasing temperature, which shows temperature sensitive magnetic property.

Moreover, the MG particles have relatively high temperature dependency as well as high saturation magnetization when compared with various types of temperature sensitive ferrite such as Ni-Zn ferrite and Mn-Zn ferrite.[23, 24]

Figure. 9 (b)-(c) shows the temperature dependency of the MG functional fluids. The magnetization values of both $Ga_{85.8}In_{14.2}$ based MG fluids and $Ga_{91.6}Sn_{8.4}$ based MG fluids decrease, which are caused by the low magnetic property of liquid metal and low solid fraction of magnetic MG particles. However, the magnetization values of the synthesized functional fluids show the temperature dependence, i.e. decrease with increase increasing temperature.

Figure. 10 shows the saturation magnetization for (a) $Fe_{73.5}Nb_3Cu_1Si_{13.5}B_9$ MG particles, (b) $Ga_{85.8}In_{14.2}$ based MG fluids and (c) $Ga_{91.6}Sn_{8.4}$ based MG fluids as a function of temperature when the magnetic flux density was kept constant at 0.8 T. We found that there is a temperature dependency of the magnetization for $Ga_{85.8}In_{14.2}$ based MG fluids and $Ga_{91.6}Sn_{8.4}$ based MG fluids within the testing temperature range of 293-333 K. Considering the temperature sensitive magnetic properties, these liquid metal-based functional fluids can be used in magneto-caloric energy conversion devices or heat exchange devices, where continuous heat diffusion and cooling can be achieved and the elastic properties can be kept at all times.[19]

Conclusion

By doping Fe-based MG particles into liquid metal alloys, we have successfully prepared $Ga_{85.8}In_{14.2}$ and $Ga_{91.6}Sn_{8.4}$-based $Fe_{73.5}Nb_3Cu_1Si_{13.5}B_9$ functional fluids. The experimental results indicate that the $Fe_{73.5}Nb_3Cu_1Si_{13.5}B_9$ particles have high saturation magnetization. As for the $Ga_{85.8}In_{14.2}$ and $Ga_{91.6}Sn_{8.4}$-based MG magnetic functional fluids, both of them exhibit good magnetization. The saturation magnetization of $Ga_{85.8}In_{14.2}$-based MG fluids is about 0.6 emu/g, which is higher than that of the $Ga_{91.6}Sn_{8.4}$-based MG fluids. $Ga_{85.8}In_{14.2}$ and $Ga_{91.6}Sn_{8.4}$-based Fe_3O_4 magnetic fluids exhibit superparamagnetism, however the saturation magnetizations of the $Ga_{91.6}Sn_{8.4}$ and $Ga_{85.8}In_{14.2}$-based Fe_3O_4 magnetic fluids are lower than

that of $Ga_{85.8}In_{14.2}$ and $Ga_{91.6}Sn_{8.4}$-based MG functional fluids. We found that both of $Ga_{85.8}In_{14.2}$ based MG fluids and $Ga_{91.6}Sn_{8.4}$ based MG fluids showed a temperature sensitive of magnetization within the testing temperature range of 293-333 K.

Considering the excellent temperature sensitive magnetic properties and fluidity as well as high thermal and electrical conductivity, these liquid metal-based magnetically controllable fluids should have potential applications in a variety of emerging applications, especially in elevated-temperature seals, high temperature cooling and magneto-caloric energy conversion devices.

Acknowledgement

The authors are grateful for the financial support from the National Natural Science Foundation of China (Grant No. 51371107) and Scientific and Technological Project of Shandong Province (Grant No.2013GGX1027).

References

[1] R. E. Rosensweig, *Ferrohydrodynamics*, Cambridge University Press: Cambridge, England **1985**.

[2] G. Jia, W. L. Yang, C. C. Wang, *Adv. Mater.* **2013**, *25*, 5196.

[3] M. Molazemi, H. Shokrollahi, B. Hashemi, *J. Magn. Magn. Mater.* **2013**, *346*, 107.

[4] C. C. Yang, X. F Bian, J. F. Yang, *Funct. Mater. Lett*. **2014**, *7*, 1450028.

[5] P. Tartaj, M. D. P. Morales, S. V. Verdaguer, T. G. Carreno, C. J. Serna, *J. Phys. D: Appl. Phys*. **2003**, *36*, 182.

[6] O. Veiseh, J. W. Gunn, M. Zhang, *Adv. Drug. Delivery. Rev*. **2010**, *62*, 284.

[7] H. Shokrollahi, *Mat. Sci. Eng. C*. **2013**, *33* 2476.

[8] Y. H. Tian, G. H. Su, J. Wang, W. X. Tian, S. Z. Qiu, *Prog. Nucl. Energ.* **2013**, *68*, 177.

[9] E. Dubois, J. Chevalet, R. Massart, *J. Mol. Liq.* **1999**, *83*, 243.

[10] T. Fujita, H. S. Park, K. Ono, S. Matsuo, K. Okaya, G. Dodbiba, *J. Magn. Magn. Mater.* **2011**, *323*, 1207.

[11] M. Xiong, Y. Gao, J. Liu, *J. Magn. Magn. Mater.* **2014**, *354*, 279.

[12] X. Wang , J. Zhuang , Q. Peng , Y. D. Li , *Nature*, **2005**, *437*, 121.

[13] S. H. Sun , C. B. Murray , D. Weller , L. Folks , A. Moser , *Science* **2000**, *287*, 1989.

[14] X. Q. Xu , C. H. Deng , M. X. Gao , W. J. Yu , P. Y. Yang , X. M. Zhang , *Adv. Mater.* **2006**, *18*, 3289.

[15] R.X. Zheng, H. Yang, T. Liu, K. Ameyama, C. L. Ma, *Mater. Design*. **2014,** *53*, 512.

[16] H. Zohdi, H. R. Shahverdi, S. M. M. Hadavi, *Electrochem. Commun*. **2011**, *13*, 840.

[17] A. Inoue, A. Takeuchi, *Acta Mater*, **2011**, *59*, 2243

[18] X. L. Zhao, X. F. Bian, Y. W. Bai, X. X. Li, *J. Appl. Phys*. **2012**, *111*, 103514.

[19] E. Auzans, D. Zins, E. Blums, R. Massart, *J. Mater. Sci.* **1999**, *34*, 1253.

[20] R. N. Singh, *J. Mater. Eng. Perform*. **2006**, *15*, 422.

[21] Y. Zheng, Z. Z. He, J. Yang, J. Liu, *Sci. Rep*. **2014**, DOI: 10.1038/srep04588.

[22] H. J. Chen, Y. M. Wang, J. M. Qu, R. Y. Hong, H. Z. Li, *Appl. Sure. Sci*. **2011**, *257*, 10802.

[23] P. Poddar, J. Gass, D. J. Rebar, S. Srinath, H. Srikanth, S. A. Morrison, E. E. Carpenter, *J. Magn. Magn. Mater.* **2006**, *307*, 227.

[24] R. Arulmurugan, G. Vaidyanathan, S. Sendhilnathan, B. Jeyadevan, *J. Magn. Magn. Mater.* **2006**, *298*, 83.

[25] Y. Zhao, J. Fang, H. X. Wang, X. G. Wang, T. Lin, *Adv. Mater.* **2010**, *22*, 707.

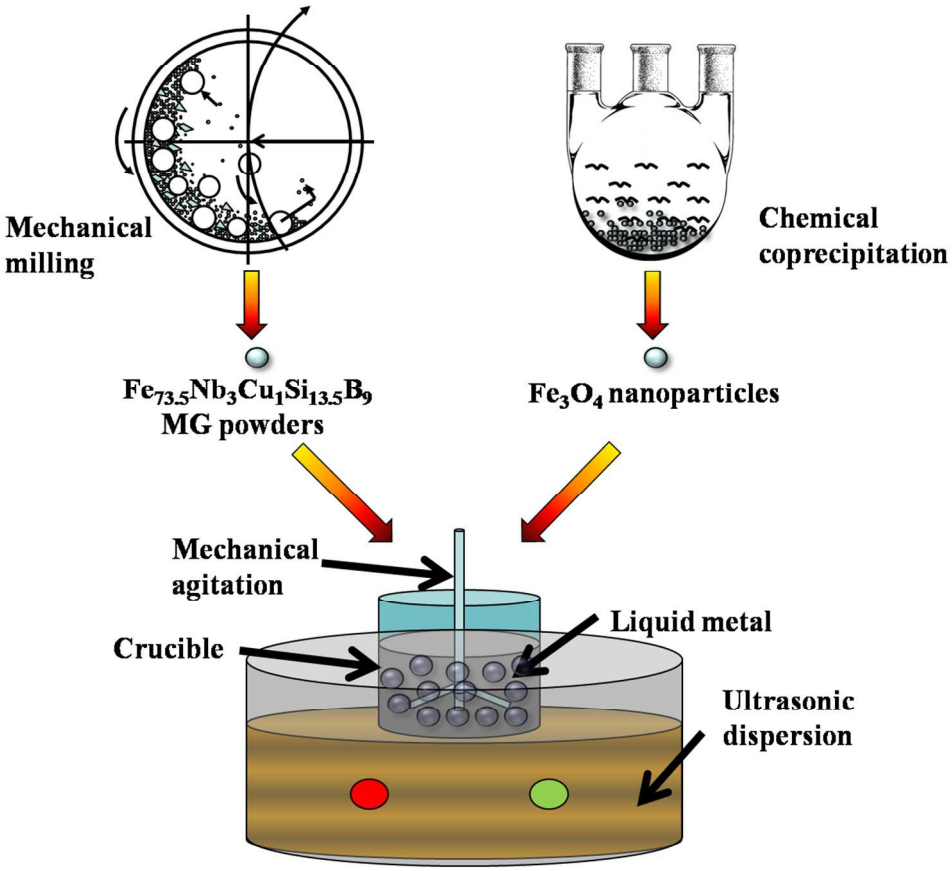

The sketch of preparation of liquid metal-based functional fluids
108x104mm (300 x 300 DPI)

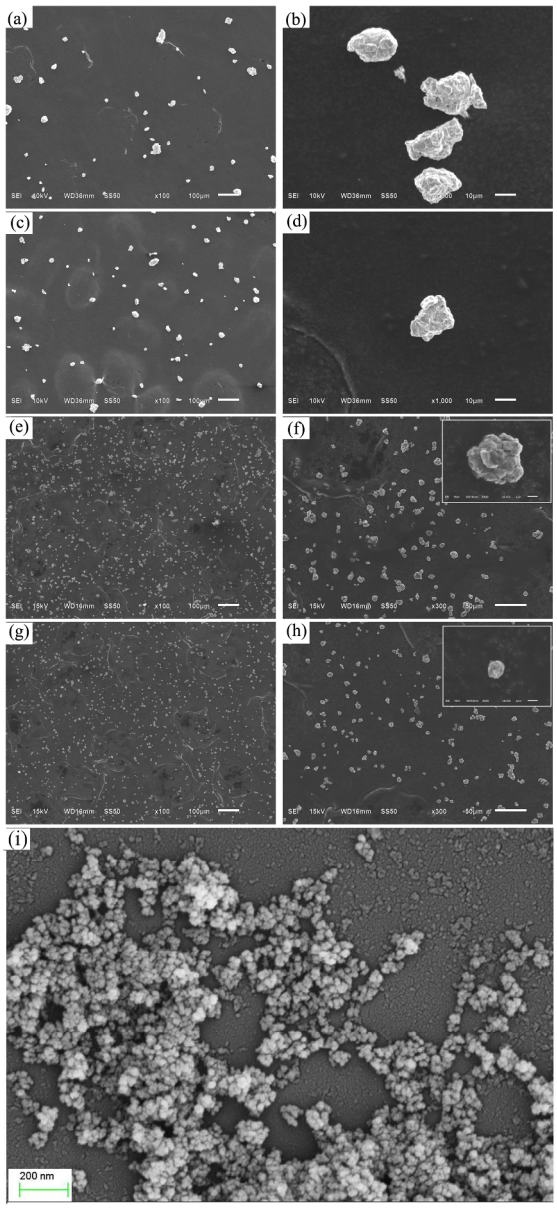

SEM images of Fe73.5Nb3Cu1Si13.5B9 MG particles and Fe3O4 nanoparticles. (a) (b) MG powders after being milled 12 h. (c) (d) MG powders after being milled 24 h. (e) (f) MG powders after being milled 36 h. (g) (h) MG powders after being milled 48 h. (i) Fe3O4 nanoparticles.
132x284mm (300 x 300 DPI)

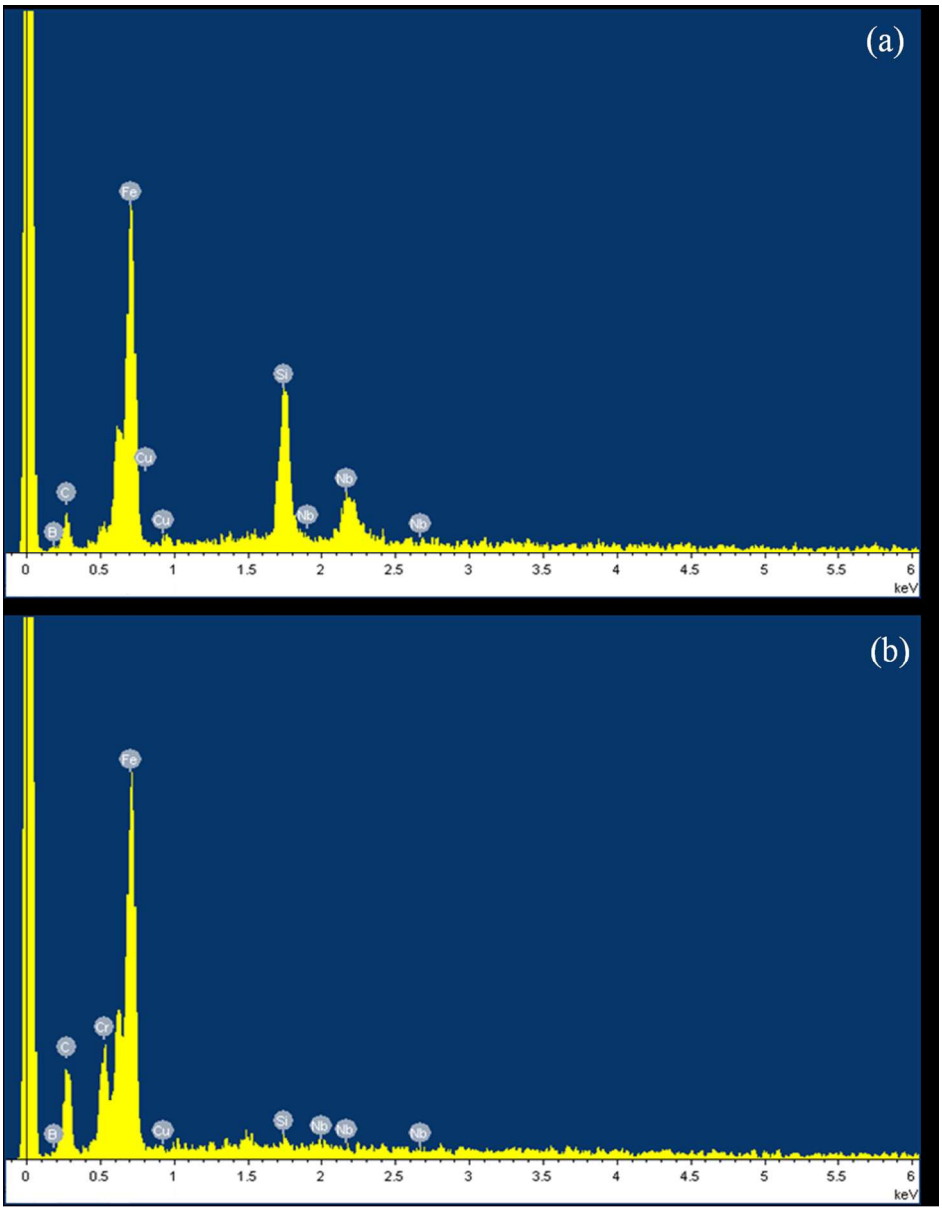

The SEM-EDX spectrograms of Fe73.5Nb3Cu1Si13.5B9 MG ribbons (a) and powders (b) after being milled for 48h.
226x291mm (150 x 150 DPI)

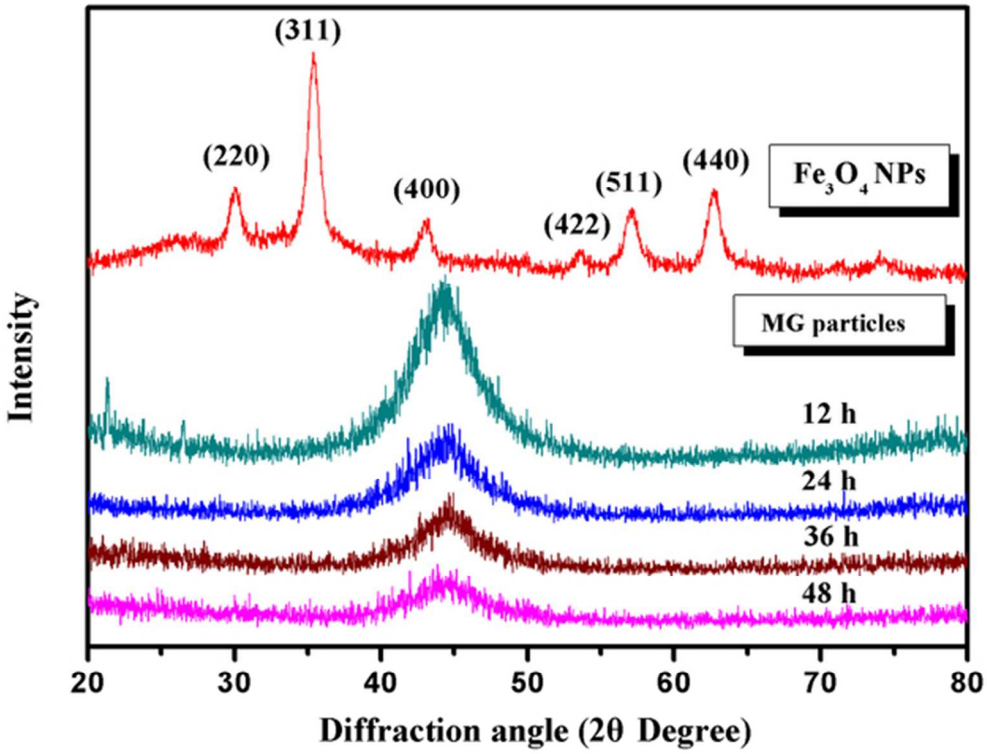

The XRD patterns of Fe3O4 nanoparticles and Fe73.5Nb3Cu1Si13.5B9 particles after being milled for 12h, 24h, 36h and 48h.
53x41mm (300 x 300 DPI)

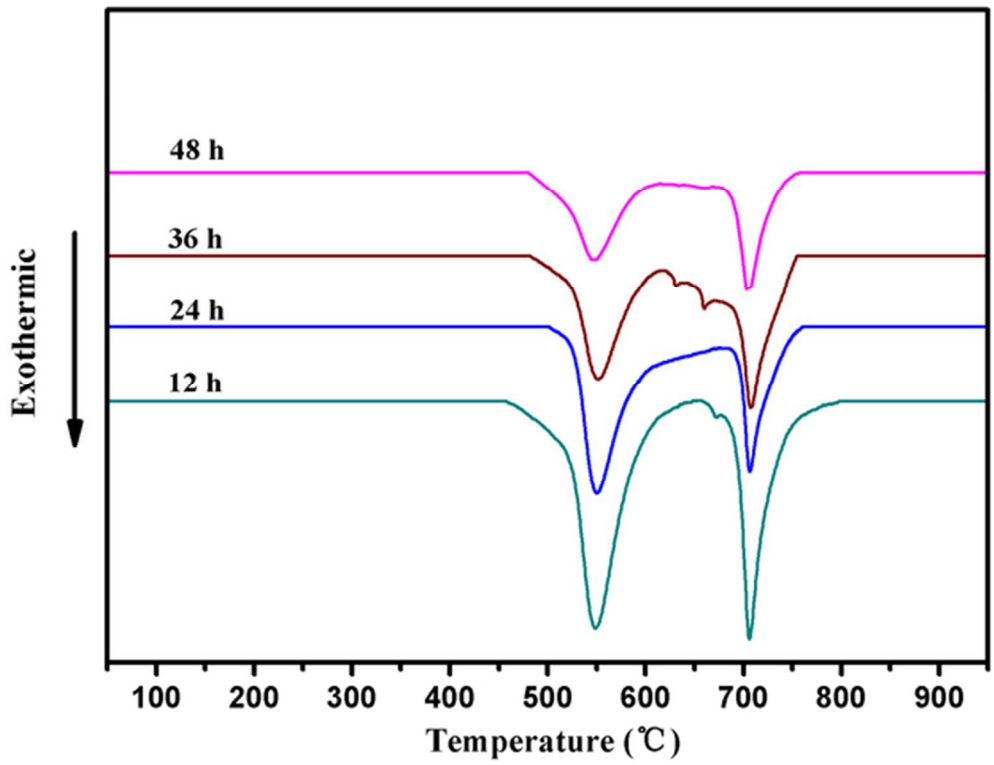

DSC curves of Fe73.5Nb3Cu1Si13.5B9 MG particles after being milled with a heating rate of 20 K/min
53x41mm (300 x 300 DPI)

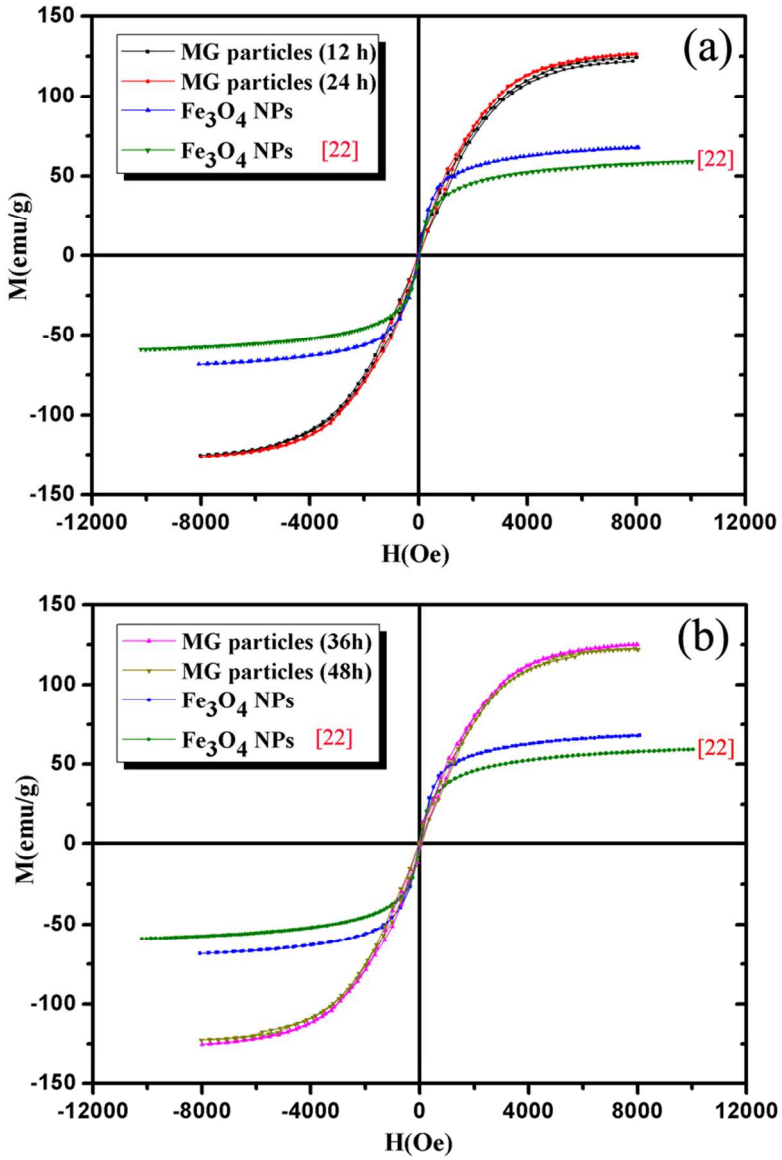

Hysteresis curves of Fe3O4 nanoparticles and Fe73.5Nb3Cu1Si13.5B9 MG particles after being milled for different hours (a) 12h, 24h. (b) 36h, 48h
74x111mm (300 x 300 DPI)

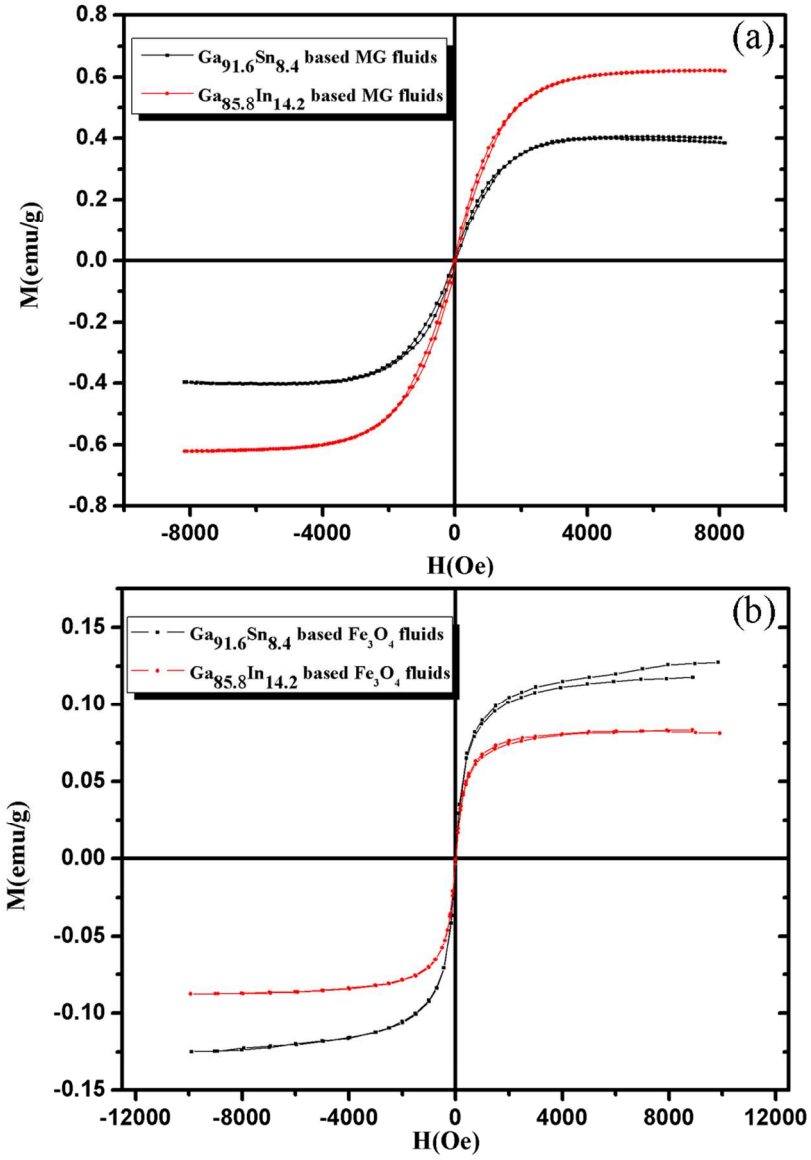

Figure. 7 Hysteresis curves of liquid metal-based Fe73.5Nb3Cu1Si13.5B9 magnetic functional fluids (a) and liquid metal-based Fe3O4 magnetic fluids (b).
95x132mm (300 x 300 DPI)

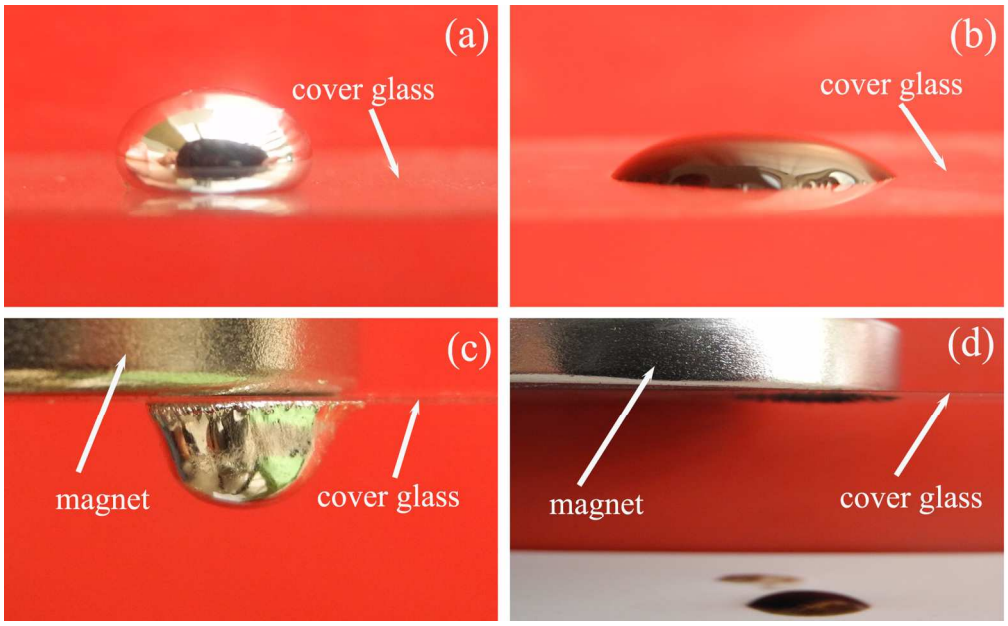

The behaviors of the fluid droplets of Ga85.8In14.2-based magnetic functional fluids (a, c) and water-based fluids (b, d).
154x94mm (300 x 300 DPI)

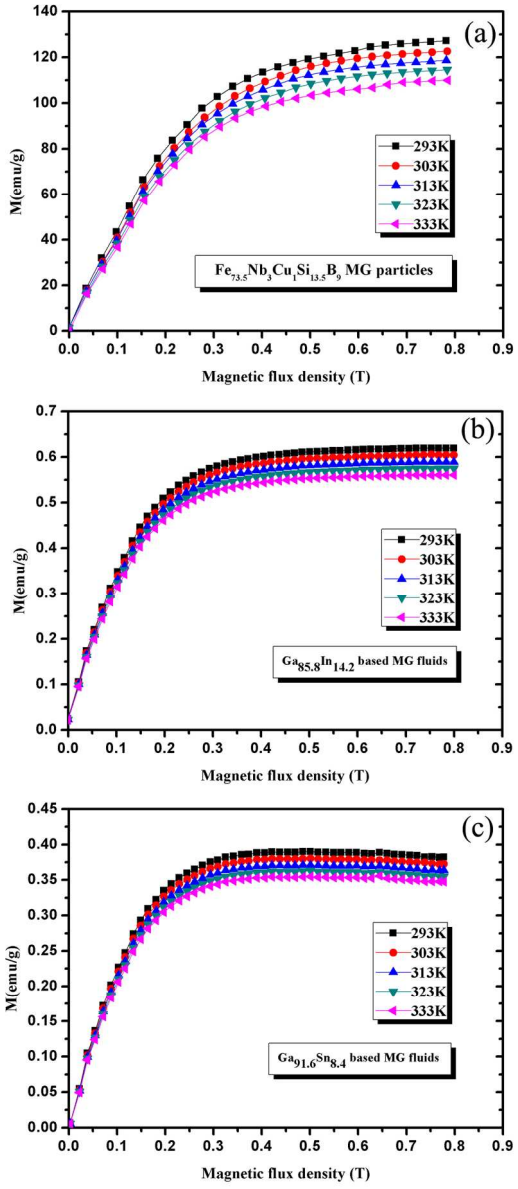

Magnetization curves of (a) Fe73.5Nb3Cu1Si13.5B9 MG particles, (b) Ga85.8In14.2 based MG fluids and (c) Ga91.6Sn8.4 based MG fluids, measured between 293 K and 333 K in 10 K steps.
89x201mm (300 x 300 DPI)

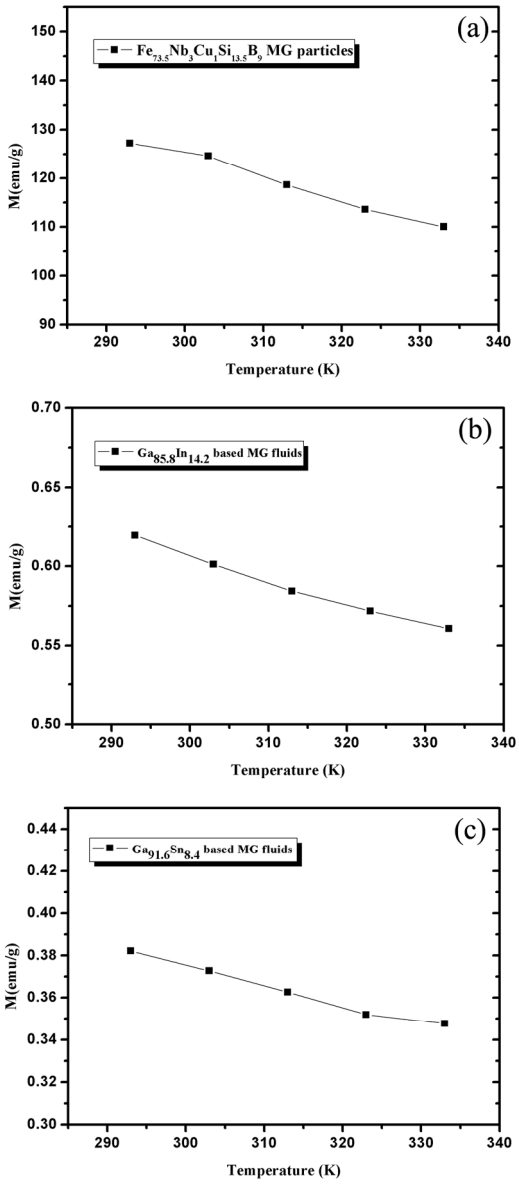

Saturation magnetization as a function of temperature for (a) Fe73.5Nb3Cu1Si13.5B9 MG particles, (b) Ga85.8In14.2 based MG fluids and (c) Ga91.6Sn8.4 based MG fluids, measured at 0.8T.
91x202mm (300 x 300 DPI)

Table.1 parameters of $Ga_{91.6}Sn_{8.4}$ and $Ga_{85.8}In_{14.2}$ based functional fluids.

Samples	Saturation magnetization (emu/g)		Coercivity (Gs)		Remanent magnetization (emu/g)	
	negative	positive	negative	positive	negative	positive
$Ga_{91.6}Sn_{8.4}$+MG	-0.39	0.40	-28.40	28.38	-0.03	0.03
$Ga_{85.8}In_{14.2}$+MG	-0.62	0.62	-24.28	-24.31	-0.04	0.04
$Ga_{91.6}Sn_{8.4}$+Fe_3O_4	-0. 13	0.13	-11.25	11.28	-0.003	0.003
$Ga_{85.8}In_{14.2}$+Fe_3O_4	-0.08	0.08	-7.14	7.13	-0.001	0.001

Figure captions

Figure.1 The sketch of preparation of liquid metal-based functional fluids

Figure. 2 SEM images of $Fe_{73.5}Nb_3Cu_1Si_{13.5}B_9$ MG particles and Fe_3O_4 nanoparticles. (a) (b) MG powders after being milled 12 h. (c) (d) MG powders after being milled 24 h. (e) (f) MG powders after being milled 36 h. (g) (h) MG powders after being milled 48 h. (i) Fe_3O_4 nanoparticles.

Figure. 3 The SEM-EDX spectrograms of $Fe_{73.5}Nb_3Cu_1Si_{13.5}B_9$ MG ribbons (a) and powders (b) after being milled for 48h.

Figure. 4 The XRD patterns of Fe_3O_4 nanoparticles and $Fe_{73.5}Nb_3Cu_1Si_{13.5}B_9$ particles after being milled for 12h, 24h, 36h and 48h.

Figure. 5 DSC curves of $Fe_{73.5}Nb_3Cu_1Si_{13.5}B_9$ MG particles after being milled with a heating rate of 20 K/min

Figure. 6 Hysteresis curves of Fe_3O_4 nanoparticles and $Fe_{73.5}Nb_3Cu_1Si_{13.5}B_9$ MG particles after being milled for different hours (a) 12h, 24h. (b) 36h, 48h

Figure. 7 Hysteresis curves of liquid metal-based $Fe_{73.5}Nb_3Cu_1Si_{13.5}B_9$ magnetic functional fluids (a) and liquid metal-based Fe_3O_4 magnetic fluids (b).

Figure. 8 The behaviors of the fluid droplets of $Ga_{85.8}In_{14.2}$-based magnetic functional fluids (a, c) and water-based fluids (b, d).

Figure. 9 Magnetization curves of (a) $Fe_{73.5}Nb_3Cu_1Si_{13.5}B_9$ MG particles, (b) $Ga_{85.8}In_{14.2}$ based MG fluids and (c) $Ga_{91.6}Sn_{8.4}$ based MG fluids, measured between 293 K and 333 K in 10 K steps.

Figure. 10 Saturation magnetization as a function of temperature for (a) $Fe_{73.5}Nb_3Cu_1Si_{13.5}B_9$ MG particles, (b) $Ga_{85.8}In_{14.2}$ based MG fluids and (c) $Ga_{91.6}Sn_{8.4}$ based MG fluids, measured at 0.8T.

Table.1 Parameters of $Ga_{91.6}Sn_{8.4}$ and $Ga_{85.8}In_{14.2}$ based functional fluids.